Inflammation Induced by MMP-9 Enhances Tumor Regression of Experimental Breast Cancer

Karin Söderlund Leifler,*,† Susanne Svensson,*,† Annelie Abrahamsson,*,†
Christina Bendrik,*,† Jennifer Robertson,‡ Jack Gauldie,‡ Anna-Karin Olsson,§ and
Charlotta Dabrosin*,†

Matrix metalloproteinases (MMPs) have been suggested as therapeutic targets in cancer treatment, but broad-spectrum MMP inhibitors have failed in clinical trials. Recent data suggest that several MMPs including MMP-9 exert both pro- and antitumorigenic properties. This is also the case of the natural inhibitors of MMPs, tissue inhibitor of metalloproteinases (TIMPs). The inhibitor of MMP-9 is TIMP-1, and high levels of this enzyme have been associated with decreased survival in breast cancer. Inflammation is one hallmark of cancer progression, and MMPs/TIMPs may be involved in the local immune regulation. We investigated the role of MMP-9/TIMP-1 in regulating innate antitumor immunity in breast cancer. Breast cancers were established in nude mice and treated with intratumoral injections of adenoviruses carrying the human TIMP-1 or MMP-9 gene (AdMMP-9). In vivo microdialysis for sampling of cancer cell–derived (human) and stroma-derived (murine) proteins, immunostainings, as well as cell cultures were performed. We report a dose-dependent decrease of tumor growth and angiogenesis after AdMMP-9 treatment. In addition to increased generation of endostatin, AdMMP-9 promoted an antitumor immune response by inducing massive neutrophil infiltration. Neutrophil depletion prior to gene transfer abolished the therapeutic effects of AdMMP-9. Additionally, AdMMP-9 activated tumor-infiltrating macrophages into a tumor-inhibiting phenotype both in vivo and in vitro. AdMMP-9 also inhibited tumor growth in immune-competent mice bearing breast cancers. Adenoviruses carrying the human TIMP-1 gene had no effect on tumor growth or the immune response. Our novel data identify MMP-9 as a potent player in modulating the innate immune response into antitumor activities.   *The Journal of Immunology*, 2013, 190: 4420–4430.

M atrix metalloproteinases (MMPs) are overexpressed in many types of cancer and have been associated with tumor progression due to their capacity to degrade the basement membrane and activate growth factors (1, 2). However, MMP inhibitors in clinical trials have failed and even induced poorer survival compared with placebo-treated patients (3). In addition to the clinical trial data, a number of experimental studies have shown potent antitumorigenic activities of several MMPs including MMP-9 (4–8). These antitumorigenic activities may be attributed to the generation of antiangiogenic fragments such as angiostatin, tumstatin, and endostatin (4–7). The natural-occurring endogenous inhibitor of MMP-9 is tissue inhibitor of metalloproteinase-1 (TIMP-1) (9). Similar to MMPs, the role of TIMPs in cancer is reported contradictory and both tumor-protective and tumor-enhancing properties have been reported (10–13). In breast cancer patients, high tumor and serum levels of TIMP-1 have been associated with decreased response to chemotherapy and decreased survival, suggesting a detrimental effect of TIMP-1 (14–16).

MMPs are involved in the local immune regulation on several levels. MMPs can shed chemokines from cellular membranes, modify soluble chemokines to alter their localization patterns or activity, and facilitate immune cell migration by basal membrane proteolysis (17, 18). Inflammation is one of the hallmarks of cancer initiation and progression (19). Infiltration of immune cells such as tumor-associated macrophages (TAMs) have a role in tumor progression; however, depending on their phenotype macrophages can have either tumor-killing (M1) or tumor-promoting (M2) properties (20, 21). However, mixed phenotypes have been detected, and subsets of macrophages may coexist in the tumor tissue as the activation of TAMs depend on signals in the microenvironment (21–24).

The role of tumor-associated neutrophils is unclear, but it seems probable that they have the ability to be pro- or antitumorigenic, depending on their phenotype or the number of infiltrating neutrophils in the tumor microenvironment (25, 26). In addition, it has been demonstrated that massive infiltration of neutrophils may elicit a cytotoxic effect, leading to tumor regression, whereas a low-grade neutrophil gradient is tumor progressive (25, 26).

We have previously shown in established breast cancer tumors in nude mice that gene transfer of MMP-9 but not TIMP-1 led to

*Division of Oncology, Department of Clinical and Experimental Medicine, Linköping University, Linköping 58185, Sweden; †Department of Oncology, County Council of Östergötland, Linköping 58185, Sweden; ‡Department of Pathology and Molecular Medicine, McMaster University, Hamilton, Ontario L8N 3Z5, Canada; and §Department of Medical Biochemistry and Microbiology, Uppsala Biomedical Centre, Uppsala University, Uppsala 75105, Sweden

Address correspondence and reprint requests to Prof. Charlotta Dabrosin, Department of Oncology, Division of Oncology, Linköping University, SE-581 85 Linköping, Sweden. E-mail address: charlotta.dabrosin@liu.se

tumor regression via increased generation of the antiangiogenic fragment endostatin (4). In this study, we investigated if gene transfer of MMP-9 affected the immune response. By using a human breast cancer model in a mouse, BALB c *nu/nu* with intact innate immunity, B cells, and NK cells but T cell–deficient, we had the possibility to delineate events occurring in the cancer cells (human) or the tumor stroma (murine). We show that gene transfer of MMP-9 to established breast cancer tumors induced tumor regression via increased neutrophil infiltration and an activation of TAMs into antitumorigenic properties, whereas TIMP-1 had no effect on the innate immunity.

Materials and Methods

Cell culture

MCF-7 (HTB-22; human breast adenocarcinoma, estrogen receptor– and progesterone receptor–positive) cells were obtained from the American Type Culture Collection (ATCC; Manassas, VA). Cells were cultured in DMEM without phenol red supplemented with 2 mM glutamine, 50 IU/ml penicillin-G, 50 μg/ml streptomycin, and 10% FBS, at 37˚C in a humidified atmosphere of 5% CO_2. Cell-culture medium and additives were obtained from Invitrogen (Carlsbad, CA) unless otherwise stated.

Adenoviral vector constructs

Adenoviral vectors containing the human gene of MMP-9 (AdMMP9), TIMP-1 (AdTIMP-1), or an empty control vector (Addl70-3) were used. The human cDNA for MMP-9 was purchased from ATCC, and the human cDNA for TIMP-1 was a gift from C. Richards (Department of Pathology and Molecular Medicine, Centre for Gene Therapeutics, McMaster University, Hamilton, ON, Canada). Both cDNAs were cloned into the loxP-containing shuttle vector, pDC316, for viral assembly. Cotransfection of recombinant pDC316 and adenovirus genomic plasmid, pBHGloxΔE1, 3Cre, subsequent purification, and amplification were carried out as previously described (4).

Animals, tumor establishment, and vector administration

All mice were housed at Linköping University, and the care and treatment conformed to the regulatory standards. The institutional animal ethics committee at Linköping University approved the study. Female, athymic mice, BALB/cA *nu/nu* (ages 4 to 5 wk) (Taconic, Ry, Denmark) and FVB/n mice (Scanbur, Sollentuna, Sweden) were housed in a pathogen-free isolation facility, light/dark cycle of 12/12 h, and fed chow and water ad libitum. Mice were anesthetized with i.p. injections of ketamine/xylazine, oophorectomized, and implanted s.c. with 3-mm pellets containing 17β-estradiol, 0.18 mg/60 d release of estradiol (Innovative Research of America, Sarasota, FL), resulting in serum concentrations of 150–250 pmol/l (27, 28). One week after surgery, MCF-7 cells (5×10^6 in 200 μl PBS) or a single-cell suspension of 0.5×10^6 cells in 200 μl PBS derived from a transgenic mouse strain expressing polyoma middle T (PyMT) Ag under the control of the mouse mammary tumor virus (MMTV) long terminal repeat were injected on the right hind-side flank in the mammary fat pad of nude mice or FVB/n mice, respectively. At a tumor size of ~40 mm^2, the mice were divided into subgroups, and the vectors AdMMP9, AdTIMP-1, or Addl70-3 were injected intratumorally at different doses. We have previously shown an efficient gene transfer with increase protein levels of the two different vectors and, in the case of MMP-9, both the protein levels and MMP-9 activity increase in vivo in this breast cancer model (4). Microdialysis was performed 7 d after adenovirus injections. Tumor volume was monitored using a caliper every 4 d.

Quantification of MMP-9 activity

As previously described, intratumoral activity of MMP-9 in vivo was quantified using a quenched fluorogenic substrate (DNP-Pro-Leu-Gly-Met-Trp-Ser-Arg-OH; Calbiochem, Merck Biosciences, Nottingham, U.K.) (6). Briefly, mice were anesthetized, and microdialysis probes (20-kDa molecular mass cutoff, 0.5-mm diameter, membrane length 4 mm; CMA/Microdialysis, Solna, Sweden) were inserted intratumorally. The microdialysis probes were perfused with 50 μmol/l MMP substrate at 2 μl/min. Microdialysates were collected at 30-min intervals into amber tubes and analyzed using a Cary Eclipse fluorescence spectrophotometer (Varian, Palo Alto, CA) with λ_{ex} at 280 nm and λ_{em} 360 nm.

In vivo inhibition of neutrophils

MCF-7 tumors were treated by intratumoral injections with 15 μg neutrophil-specific rat anti-mouse Ly-6G Ab (clone 1A8, IgG 2a,κ; BD Pharmingen, San Jose, CA) or the isotype-matched control rat IgG2a,κ (BD Pharmingen) 48 h before and after MMP-9 intratumoral gene transfer.

Microdialysis

Tumor-bearing mice were anesthetized with an i.p. injection of ketamine/xylazine and kept anesthetized by repeated s.c. injections of ketamine/xylazine. Body temperatures were maintained by heating lamps. Microdialysis probes (CMA/20 0.5-mm diameter; PES membrane length 4 mm, 100-kDa cutoff; CMA/Microdialysis) were inserted into tumor tissue and connected to a CMA/102 microdialysis pump (CMA/Microdialysis) perfused at 0.6 μl/min with Voluven 60% (Fresenius Kabi, Uppsala, Sweden). After a 60-min equilibrium period, outgoing perfusates were collected on ice and stored at −70˚C for subsequent analysis.

Quantification of proteins in microdialysates and cell-culture media

Microdialysates and culture media were analyzed with immunoassays from R&D Systems (Minneapolis, MN) unless otherwise stated: human endostatin (Quantikine), murine endostatin (murine ELISA kit; Uscn life Science, Wuhan, China), human vascular endothelial growth factor (VEGF; QuantiGlo), and murine VEGF (mouse VEGF; Quantikine). Human IL-1α, IL-1β, IL-6, IL-8, IL-10, IL-12, and TNF-α were analyzed using Human Fluorokine MAP kits with corresponding bead kits and analyzed on a Luminex 100 System (Luminex, Austin, TX). IL-1Ra (human IL-1Ra; Quantikine ELISA kit; Quantikine). The murine cytokines IL-1β, IL-10, keratinocyte chemoattractant (KC), and MIP-2 were analyzed using the Murine Fluorokine MAP base kit with corresponding beads kits and on a Luminex 100 System (Luminex); murine IL-6, IL-1Ra, and TNF-α using Murine Quantikine ELISA kits (Quantikine); and arginase-1 ELISA (Nordic BioSite, Täby, Sweden). Assays were conducted according to the manufacturer's guidelines.

Immunohistochemistry

Formalin-fixed, paraffin-embedded tumors were cut in 3- or 4-μm sections, deparaffinized, and subjected to immunohistochemistry, rabbit anti-human von Willebrand (dilution 1:1000; DakoCytomation, Carpinteria, CA), rat anti-mouse Pan-NK cells marker at 10 μg/ml (clone DX5; eBioscience, San Diego, CA), rat anti-mouse F4/80 at 0.67 μg/ml (clone CI:A3-1; Abcam, Cambridge, MA), rat anti-mouse Ly6G at 1.25 μg/ml (clone 1A8; BD Pharmingen), rabbit anti-human MMP-9 at 10 μg/ml (Chemicon, Hampshire, U.K.), or rabbit anti-human caspase-3 (dilution 1:50; Abcam) and counterstained with Mayer's hematoxylin. Negative controls did not show staining. All evaluation was performed in a blinded manner. Images of hot-spot areas of three to five tumors in each treatment group were acquired on an Olympus BX41 microscope coupled to an Olympus DP70 CCD camera (Olympus). The images were digitally analyzed, and percentage of area positively stained was quantified using ImageJ software version 1.42q (National Institutes of Health, Bethesda, MD) and CellSense (Olympus). Neutrophils and NK cells were counted in three hot-spot areas of four individual tumors.

Immunofluorescence

Deparaffinized 4-μm tumor sections were incubated with Abs against mouse F4/80 and the mouse mannose receptor-1 (MRC1) (clone 15-2; Abcam), exposed to conjugated Abs (Alexa Fluor 546 and 488), and mounted using SlowFade Gold with DAPI (Invitrogen, Eugene, OR). Samples were visualized using an Olympus BX41 light/fluorescence microscope ($\times$40/0.75; Olympus), excitation filters 495–519 nm and 556–573 nm, and an Olympus DP70 CCD camera (Olympus).

Gene transfer of cultured monocytes

Human heparin blood was diluted with RPMI medium and separated over a Ficoll paque gradient (GE Healthcare) for 30 min at 1500 rpm. The interface was washed, and 0.7×10^6 cells/well in 24-well plates was seeded in RPMI medium with 5% FBS and penicillin/streptomycin and incubated for 2 h at 37˚C. Adherent monocytes were cultured for 3 d and then treated with AdMMP-9, AdTIMP-1, or Addl70-3 at 100 PFU/cell at 37˚C for 2 h; thereafter, 250 μl medium was added. After 24 h, medium was collected, centrifuged, and frozen for subsequent analysis. The regional ethical review board of Linköping approved the plasma sampling and consent procedure. The donors gave verbal informed consent before venipuncture. Written informed consent is not mandatory by the ethical vetting in Sweden. The consent was documented in the research files, and the samples were decoded and treated anonymously thereafter. The study was conducted according to the principles expressed in the Declaration of Helsinki.

Murine macrophages (CRL-2278; ATCC) were seeded, 0.5×10^6 cells/cm², on 24-well plates in RPMI medium with 5% FBS and penicillin/streptomycin. After 24 h, the protease-activated receptor (PAR)-1 antagonist SCH79797 (Tocris Bioscience, Bristol, U.K.) or the PAR-2 antagonist ENMD-1068 (ENZO Life Science, Skärholmen, Sweden) was added for 3 h, and thereafter, 100 PFU/cell AdMMP-9 or Addl70-3 was added for 2 h. Thereafter, fresh medium containing the PAR antagonists was added. After 24 h, medium was centrifuged and frozen for subsequent analysis.

Gene transfer of human neutrophils

Neutrophils from human heparin blood were separated over a Percoll gradient (GE Healthcare) for 25 min at 1500 rpm. The interface containing neutrophils was washed and 0.5×10^6 cells diluted in HBSS with 20% autologous complete serum and transferred to sterile 2-ml polypropylene tubes. Cells were treated with AdMMP-9 or Addl70-3 at 100 PFU/cell for 60 min at 37°C, washed, and incubated in HBSS/5% FBS for 20 h. Medium was collected, centrifuged, and frozen for subsequent analysis.

Statistical analyses

Data are expressed as means ± SEM. The Student t test was used unless otherwise stated. One-way ANOVA with Bonferroni post hoc test were used where appropriate. All tests were two-sided. GraphPad Prism 5.0 was used for all statistical analyses (GraphPad Software, San Diego, CA).

Results

MMP-9 gene transfer induced massive neutrophil infiltration and activation of macrophages, whereas TIMP-1 had no effect

With intratumoral injection of the adenovirus vectors, all cells present in the tumor, cancer cells as well as the stroma cells, will be subjected to gene transfer. The important end result of MMP-9 gene transfer is actual MMP-9 activity in the extracellular space. By using an in vivo activity–detection method, we were able to quantify actual enzymatic MMP-9 activity in the extracellular space in situ 1 wk after gene transfer. At 60 min of perfusion of the substrate in live tumor tissue, the MMP-9 activity in vivo significantly increased from 27,792 ± 3,240 relative fluorescence units in the control group to 38,088 ± 1,564 in the AdMMP-9–treated animals; $p < 0.05$. These are not supraphysiological levels, as we previously have shown that MMP-9 enzymatic activity after tamoxifen treatment in the same tumor model results in an increase in the same range (6). One week after gene transfer, no necrotic areas were detected on tumor sections from either treatment group.

MMP-9 but not TIMP-1 gene transfer induced significant tumor regression compared with control tumors (Fig. 1A). The AdMMP-9–treated tumors also exhibited decreased vessel density compared with the other two groups (Fig. 1A). In a subset of larger tumors (80 mm²) treated with AdMMP-9, four out of four responded with tumor stasis/regression.

At microscopy, we noticed a distinct infiltration of immune cells into the AdMMP-9–treated tumors but not in the AdTIMP-1–treated tumors. This led us to perform immunohistochemistry for detection of the various immune cells present in this tumor model. In the AdMMP-9–exposed tumors, we found a massive infiltration of neutrophils into the tumor stroma, which exhibited significantly higher number of neutrophils compared with tumors treated with the control vector or TIMP-1 vector (Fig. 1B). The major part of the stroma consisted of macrophages, ~10% of the tumor area stained positive for macrophages. However, staining with the Pan-macrophage marker F4/80 revealed no differences with either treatment (Fig. 1C). As macrophages may be activated into different phenotypes, we sought to investigate if our treatments affected the type of macrophages in the tumors. We therefore stained the tumor sections using the M2 marker MRC1. This revealed that AdMMP-9–treated tumors exhibited significantly increased levels of M1 macrophages as the staining of MRC1⁺/F4/80⁺ macrophages decreased (Fig. 1D). There were very few NK cells in the tumors without any differences between the groups

(data not shown). To investigate the time course of the events leading to tumor regression, we performed immunohistochemistry of MMP-9 expression, neutrophils, angiogenesis, and apoptosis in tumors harvested 1 and 3 wk after AdMMP-9 treatment. Adenoviral gene transfer results in a transient overexpression of the transgene in the tissue lasting 6–10 d (29). In line with this, we found intense staining of MMP-9 in tumors 1 wk after gene transfer, whereas the tumors 3 wk after gene transfer exhibited weaker staining; 12 out of 12 sections in 1-wk tumors compared with 2 out of 12 in 3-wk tumors; $p < 0.001$. Neutrophil number was also higher in 1-wk tumors compared with 3-wk tumors and along with neutrophil infiltration in the 1-wk tumors angiogenesis decreased and apoptosis increased (Fig. 1E). This suggests that MMP-9 gene transfer results in an early decline in angiogenesis and increased apoptosis. After 3 wk, there was a further slight decrease of angiogenesis concomitant with a potent increase in apoptosis, suggesting that both angiogenesis and apoptosis occurs early, but the full effect on apoptosis is a later event during tumor regression.

MMP-9 gene transfer affected the cytokine profile in live tumor tissue

To further investigate possible changes of the tumor stroma, we employed microdialysis to sample extracellular proteins in vivo to determine cytokine profiles in live tumor tissues 1 wk after gene transfer. Tumor hypoxia may be one factor that could change the microenvironment; therefore, we performed microdialysis on size-matched tumors without any visible necrotic areas 1 wk after gene transfer (i.e., early changes after gene transfer were detected) (30). From the stroma compartment (murine), we found significant increase of IL-1β and IL-6 and a significant decrease of IL-10 in the microdialysates of AdMMP-9–treated tumors (Fig. 2). The levels of the naturally occurring inhibitor of IL-1s, IL-1Ra, were also significantly increased in the AdMMP-9–treated tumors. As we detected high levels of neutrophils in the MMP-9 exposed tumors we also measured the chemokines KC and MIP-2 in the microdialysates. Indeed, we found significantly increased levels of both proteins in the AdMMP-9–treated tumors (Fig. 2). AdTIMP-1 did not change the levels of either cytokines compared with the control vector (Fig. 2). Arginase-1, IL-12, and TNF-α were not possible to detect in microdialysis samples.

MMP-9 gene transfer of cultured monocytes and neutrophils

Although the stroma does contain several cell types, staining of our tumors exhibited macrophages as a major component of this department. Therefore, we focused on these cells in vitro. Murine macrophages were transfected with the different adenovirus vectors. Throughout there were no significant changes after addition of the control vector compared with cultures without the vector. After AdMMP-9 gene transfer, the levels of TNF-α and IL-1Ra increased significantly (Fig. 3A). The levels of IL-10 showed a tendency to decrease, although no significant changes were detected (Fig. 3A). Similar to our in vivo finding, MIP-2 increased significantly after AdMMP-9 treatment (Fig. 3A); however, KC was not detectable in the cell-culture samples. The PAR, especially PAR-1 and to a lesser extent PAR-2, have been shown to be involved in the differentiation of monocytes and mediate distinct regulatory functions of these cells (31). As PAR-1 has been shown to be a substrate for MMPs including MMP-9 (32), we investigated if these receptors were affected by our MMP-9 treatment. After blocking the receptors, the levels of TNF-α and MIP-2 decreased to some extent in a dose-dependent manner (Fig. 3A, 3B). This suggests that these receptors may be one of the mechanisms involved in the MMP-9 activation of the macrophages. IL-1β and
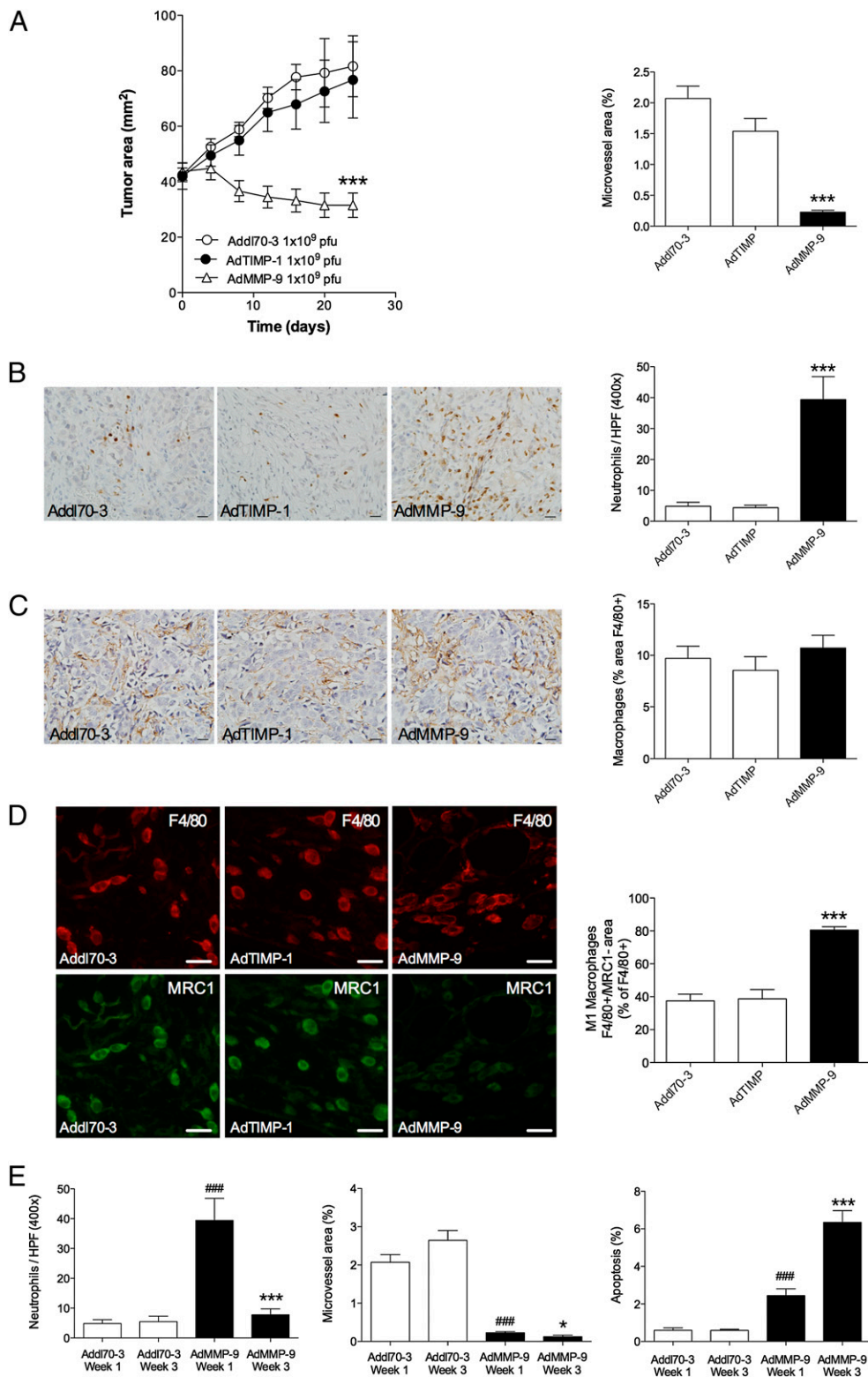
FIGURE 1. Gene transfer of MMP-9– but not TIMP-1–induced tumor regression, neutrophil infiltration, and macrophage activation in breast cancer. Nude mice were oophorectomized and supplemented with a physiologic level of estradiol. MCF-7 cells were injected s.c., and tumors were formed on the right hind flank. At similar tumor sizes (~40 mm^2), intratumoral gene transfer by adenovirus was performed with Addl70-3 (empty control vector), MMP-9, or TIMP-1 at 1×10^9 PFU. (**A**) Tumor growth and microvessel area measured after staining with anti–von Willebrand factor as described in the *Materials and Methods* section; $n = 4$–14 in each group; ANOVA, Bonferroni post hoc test. ***$p < 0.0001$. (**B**) AdMMP-9 resulted in significantly increased infiltration of neutrophils (rat anti-mouse Ly6G stained with DAB) compared with the control group and the AdTIMP-1–treated tumors; $n = 15$ in each group; ANOVA, Bonferroni post hoc test. Scale bars, 20 μm.***$p < 0.0001$. (**C**) There were no differences in stained area of the Pan-macrophage marker F4/80 (rat anti-mouse F480, DAB) in the various treatment groups; $n = 12$ in each group, ANOVA, Bonferroni post hoc test. Scale bars, 20 μm. (**D**) Staining with F4/80 (red) and the M2 marker MRC1 (green) and quantification of the number of M1 macrophages (F4/80$^+$ macrophages/MRC1$^-$); $n = 8$ in each group, ANOVA, Bonferroni post hoc test. Scale bars, 20 μm. ***$p < 0.0001$; $n = 8$ in each group. (**E**) Quantifications of immunohistochemistry sections of tumors harvested 1 and 3 wk after AdMMP-9 treatment. *$p < 0.05$, ***$p < 0.0001$ compared with AdMMP-9 wk 1, $^{###}p < 0.0001$ compared with Addl70-3 wk 1.
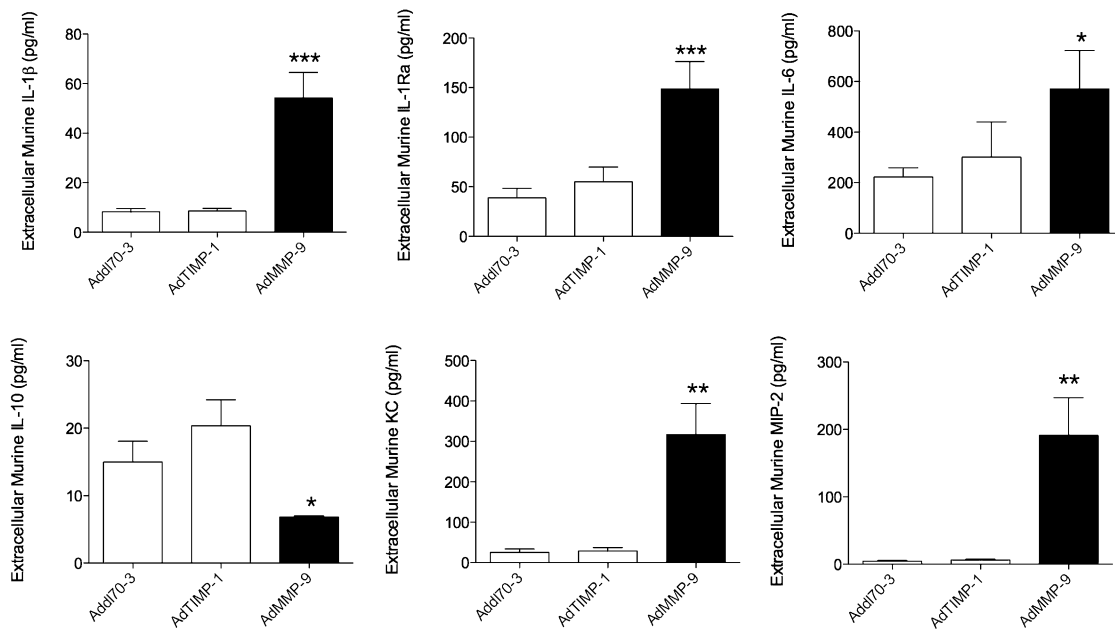
FIGURE 2. MMP-9 gene transfer but not TIMP-1 altered the cytokine profile and increased KC and MIP-2 in live tumor tissue. Nude mice were oophorectomized and supplemented with a physiologic level of estradiol. MCF-7 cells were injected s.c., and tumors were formed on the right hind flank. At similar tumor sizes (~40 mm^2), intratumoral gene transfer by adenovirus was performed with Addl70-3 (empty control vector), MMP-9, or TIMP-1 at 1×10^9 PFU. One week after virus injections, mice were anesthetized and subjected to intratumoral microdialysis for sampling of cytokines directly in vivo in tumor tissue. $n = 5$–10 in each group, ANOVA, Bonferroni post hoc test.*$p < 0.05$, **$p < 0.01$, ***$p < 0.0001$ compared with control.

IL-12 were not detectable in the culture media from these cells. As the murine macrophages are derived from virus-induced leukemia in the animals and an immortalized cell line, we next wanted to investigate if MMP-9 could induce similar polarization in freshly isolated healthy human monocytes. AdMMP-9 exposure to human macrophages corroborated our in vivo microdialysate data from breast cancer tumors with significantly increased levels of IL-1β, IL-1Ra, IL-8, and IL-6 and decreased levels of IL-10 as shown in Fig. 4. TNF-α, not detectable in microdialysates, decreased significantly (Fig. 4A). Arginase-1 and IL-12 were below the detection levels. As neutrophils were present in the tumors, we also investigated if AdMMP-9 altered the levels of cytokines from this cell type. Indeed, cultured neutrophils increased the secreted

levels of IL-1β, IL-1Ra, and IL-8 after AdMMP-9 treatment (Fig. 4B).

MMP-9 gene transfer induced a dose-response effect on breast cancer growth

Next, we set up an experiment to further investigate if the tumor-suppressive role of MMP-9 was dose dependent or whether low or high expression of MMP-9 induces tumor progression or tumor regression. We found that a low dose of the vector, 0.5×10^9 PFU, into the tumors induced tumor stasis, whereas a high dose, 2×10^9 PFU, resulted in significant tumor regression (Fig. 5A). At the end of the experiment, there was a significant difference in tumor size between low-dose– and high-dose–treated tumors (Fig. 5A). There
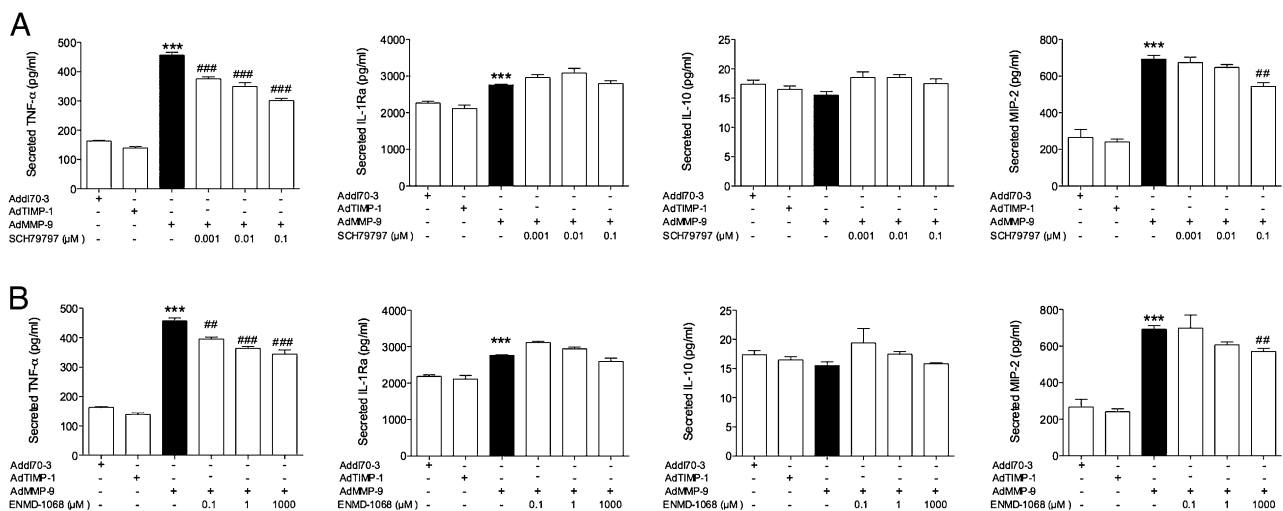

FIGURE 3. The effects of MMP-9 gene transfer were mediated by PAR-1 and PAR-2 receptors in cultured murine macrophages in vitro. Murine macrophages were cultured in vitro and transfected with Addl70-3 (empty control vector), MMP-9, or TIMP-1 at 100 PFU/cell with and without PAR-1 and PAR-2 inhibitors at different concentrations. PAR-1 inhibitor SCH79797 (**A**) or the PAR-2 inhibitor ENMD-1068 (**B**) at different concentrations. $n = 4$ in each group, ANOVA, Bonferroni post hoc test. ***$p < 0.0001$ compared with control, ##$p < 0.01$ compared with AdMMP-9, ###$p < 0.001$.
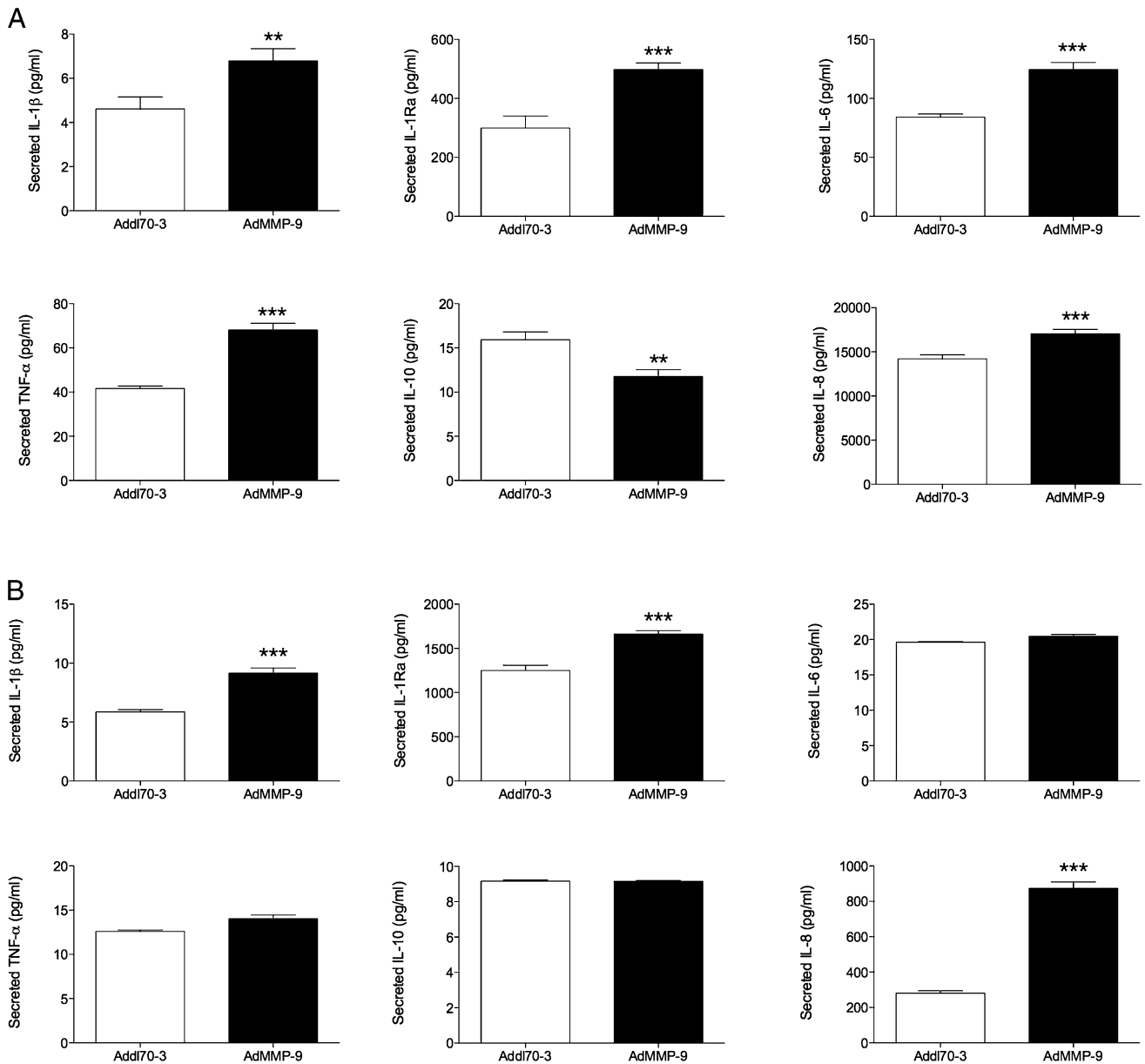
FIGURE 4. Effects of MMP-9 gene transfer on cultured human macrophages and neutrophils in vitro. (**A**) Cultured freshly isolated human macrophages exposed to AdMMP-9. $n = 8$ in each group. $**p < 0.01$, $***p < 0.0001$ compared with control. (**B**) Cultured freshly isolated human neutrophils exposed to AdMMP-9. $n = 4$ in each group. $***p < 0.0001$ compared with control.

was also a significant change of tumor angiogenesis between the two doses of MMP-9 (Fig. 5A). There was no dose-dependent response in the two control groups treated with either 0.5×10^9 or 2×10^9 PFU of the empty control vector. To further evaluate if the changes in tumor response were attributable to changes in soluble angiogenesis regulators in vivo, we performed microdialysis in size-matched tumors 1 wk after gene transfer. There was a significant increase in endostatin generation in MMP-9–treated tumors compared with controls, but there was no dose-response relationship between the two groups (Fig. 5B). There was also a slight but not significant increase of extracellular VEGF without any differences between the doses of MMP-9 (Fig. 5B).

The number of infiltrating neutrophils was significantly higher in the AdMMP-9– treated tumors with a dose-response effect by the AdMMP-9 vector (Fig. 5C). This was further supported by a significant increase of the neutrophil attractants KC and MIP-2 after AdMMP-9 therapy (Fig. 5C). MIP-2 exhibited a dose-dependent

significant increase after AdMMP-9 treatment (Fig. 5C). There were no changes in total macrophage area between the two doses of MMP-9, $11.6 \pm 0.9\%$ area in the control group and 11.5 ± 2.1 and $12.2 \pm 1.2\%$ in the low- and high-dose AdMMP-9, respectively. However, the extracellular cytokine profile in vivo after AdMMP-9 exhibited a dose-dependent increase of IL-1β, IL-1Ra, and IL-6 and a decrease of the IL-10 levels (Fig. 5D).

MMP-9 gene transfer increased neutrophil infiltration and inhibition of neutrophil activity diminished the therapeutic effect of MMP-9

As there was a dose-dependent infiltration of neutrophils into tumors treated with AdMMP-9 (Fig. 5C), with high levels in the high-dose group with potent tumor regression and lower levels in the low-dose group with less effects on tumor growth, we hypothesized that neutrophils affected tumor growth, and therefore, neutrophil depletion would modulate the therapeutic effects of
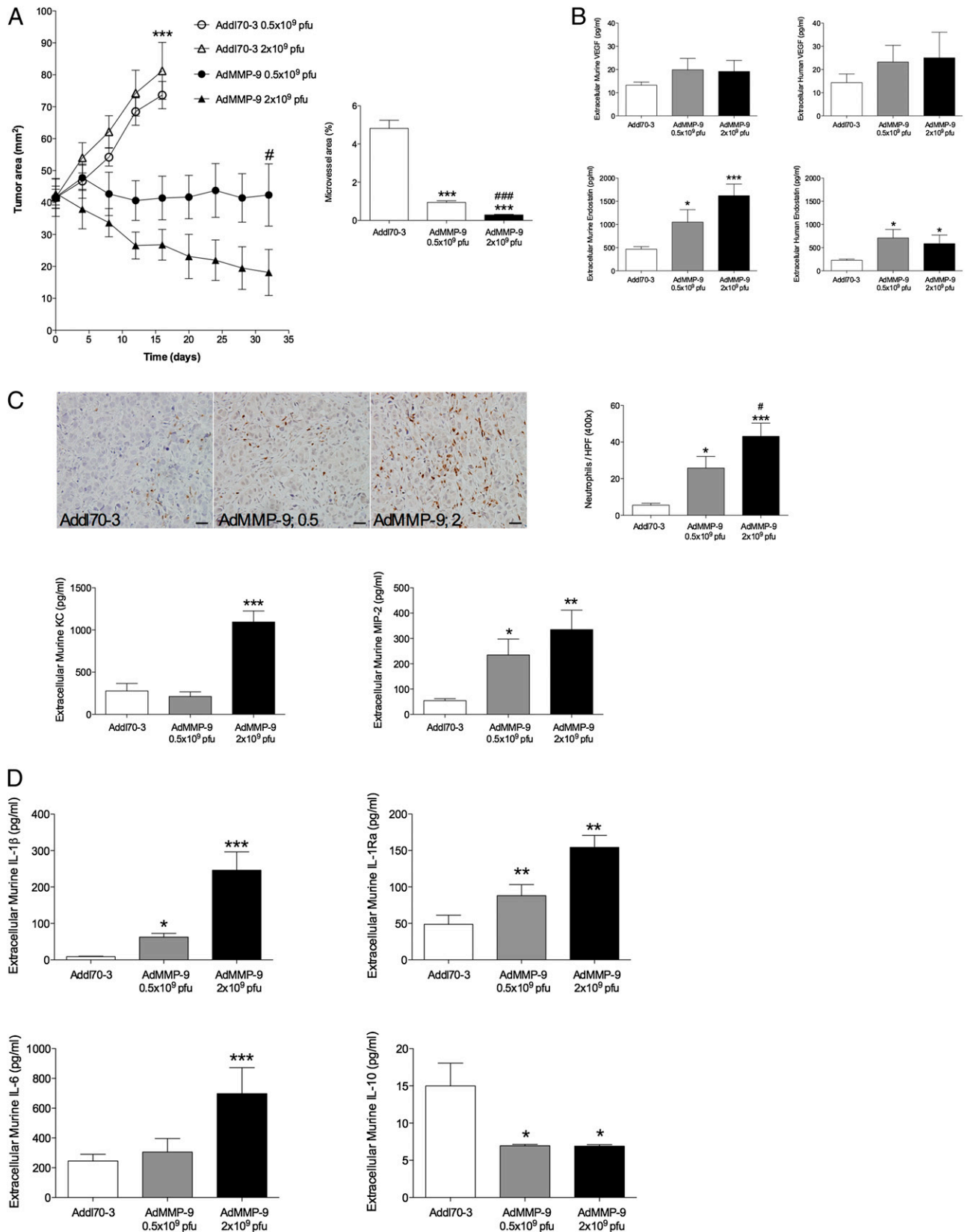
FIGURE 5. Dose-dependent effects of MMP-9 gene transfer. Nude mice were oophorectomized and supplemented with a physiologic level of estradiol. MCF-7 cells were injected s.c., and tumors were formed on the right hind flank. At similar tumor sizes (~40 mm^2), gene transfer by adenovirus was performed at different concentrations, PFU, with Addl70-3 (empty control vector) or AdMMP-9 vector. (**A**) Dose-dependent effects on tumor growth and microvessel area by AdMMP-9. AdMMP-9 decreased tumor growth in a dose-dependent manner; ***$p < 0.0001$; AdMMP-9 0.5×10^9 PFU and AdMMP-9 2×10^9 PFU versus control; $n = 6$–12, ANOVA, Bonferroni post hoc test. #$p < 0.05$, AdMMP-9 0.5×10^9 PFU versus AdMMP-9 2×10^9 PFU; $n = 6$–8, t test. Quantification of microvessel area using staining for von Willebrand factor revealed decreased microvessel area between the treatment groups. $n = 15$, ANOVA, Bonferroni post hoc test. AdMMP-9 versus control, ***$p < 0.0001$, $n = 15$ and AdMMP-9 0.5×10^9 PFU versus (*Figure legend continues*)

AdMMP-9. We injected the neutrophil-inhibiting mAb Ly6G or the isotype-matched control Ab directly into the tumors using a previously described approach (25). This neutrophil inhibition counteracted the therapeutic effect of AdMMP-9 gene transfer, confirming the role of neutrophil infiltration as one of the mechanisms of the therapeutic effects of AdMMP-9 in this tumor model (Fig. 6A), and using immunohistochemistry, we confirmed that the anti-Ly6G treatment depleted neutrophil infiltration into the tumors almost completely (Fig. 6B). Neutrophils may also be a source of MMP-9. However, anti–MMP-9 immunohistochemistry revealed no differences of staining intensity between tumor with or without neutrophil depletion with anti-Ly6G. Three randomly selected areas of four separate tumors in each treatment group were scored, and representative sections are shown in Fig. 6C.

MMP-9 gene transfer induced tumor regression and neutrophil infiltration in immune-competent mice bearing breast cancer

To elucidate whether the changes seen in nude mice were valid also in animals with an intact immune system, MMTV-PyMT breast cancer tumors were established in syngeneic FVB mice. Despite a much faster growth rate of MMTV-PyMT tumors compared with MCF-7 tumors in nude mice, AdMMP-9 gene transfer induced a similar tumor response in these two breast cancer models. Neutrophil infiltration was also similar in the two models after AdMMP-9 gene transfer (Fig. 7).

Discussion

In this study, we show previously unrecognized effects of MMP-9 on innate antitumor immunity. Adenoviral gene transfer of MMP-9 caused a dose-dependent massive infiltration of neutrophils into breast cancers, which resulted in decreased tumor growth and angiogenesis of breast cancer explants in nude mice and immune-competent mice bearing breast cancers. When the neutrophils were depleted by Ab treatment, the therapeutic effect of AdMMP-9 was abolished. In addition, AdMMP-9 treatment altered the cytokine profile of the stroma in vivo. One major component of the stroma was macrophages, and gene transfer of MMP-9 to cultured macrophages induced a similar cytokine profile, as we had detected from the stroma of the tumors. By using PAR-1 and PAR-2 inhibitors, the cytokine profile of the macrophages after AdMMP-9 exposure was to some extent altered, suggesting that these receptors may, at least in part, mediate the effects of MMP-9. AdMMP-9 exposure to cultured neutrophils altered the levels of released cytokines, suggesting that these cells may also contribute to the change in cytokine levels in the tumors. Gene transfer of TIMP-1 did not affect tumor growth, angiogenesis, or the immune cells.

MMPs have a complex role in cancer progression and may exert both pro- and antitumorigenic activities (3, 33–35). Although MMP expression generally has been associated with tumor progression in several cancer forms including breast cancer (36),

clinical trials with broad-spectrum MMP inhibitors have failed, and in some cases, patients treated with the inhibitors even showed significantly poorer survival than patients receiving placebo (3). These results are further supported by recent data showing unfavorable effects of TIMP-1 in breast cancer patients (14–16). Moreover, recent data, including MMP-9 knockout mice, has clearly shown MMP-9 may be involved in tumor regression (5). In line with these data, it has recently been shown that gene transfer of MMP-9 in combination with oncolytic viruses leads to regression of prostate cancer growth (37). One explanation may be that clinical investigations have been focused on immunohistochemistry or mRNA quantifications, which may reflect the intracellular content but not the enzymatic activity of the MMP, as these proteins are activated at a posttranslational level in the extracellular space. We, and others, have shown that increased expression of MMP-9 induces a potent and significant antitumor effect by increasing the release of antiangiogenic fragments such as endostatin (4–6). Interestingly, in vitro data implicate MMP-9 as a potent enzyme for releasing soluble VEGF and thereby involved in the angiogenic switch during cancer progression (38). Indeed, our in vivo data using microdialysis for sampling of free VEGF from the extracellular space in live tumor tissue suggest an increase of free VEGF by MMP-9; however, this effect was not significant and did not result in increased angiogenesis. This may be explained by a simultaneous increase of released endostatin, leading to a net result of antiangiogenesis in the tissue.

The MMP-9–treated tumors exhibited profound changes in the tumor stroma with high numbers of infiltrating immune cells. The secreted cytokine pattern of cells in vivo are difficult to explore with traditional methods such as immunohistochemistry and/or flow sorting of whole tumor tissue not differentiating between intracellular/extracellular molecules. Therefore, we performed microdialysis, which we previously have shown to be an excellent tool for sampling of extracellular proteins in vivo (39–44). In the tumor model used in this study with human cancer cells in a murine stroma, we were able not only to sample cytokines in vivo, but also to distinguish from which compartment of the tumor microenvironment the secreted cytokines originated. In the AdMMP-9–treated tumors, we found increased levels of murine IL-1β, IL-1Ra, and IL-6 and decreased levels of IL-10. One major component of the stroma in our tumors was macrophages. TAMs may affect tumor progression and metastasis formation (20). However, TAMs may be polarized into different phenotypes that are either beneficial or detrimental for cancer growth (45). Classically, macrophages may be polarized into M1 and M2 phenotypes depending on their cytokine profile. In a simplistic manner, M1 macrophages secrete low levels of arginase-1 and IL-10 and high levels of IL-1β, IL-6, TNF-α, and IL-12, whereas M2 macrophages secrete high levels of arginase-1, IL-10, and IL-1Ra and low levels of IL-12, IL-1β, IL-6, and TNF-α (45). However, great heterogeneity and plasticity of the macrophage skewing has been found, and the typical M1 and M2 state has been considered ex-

---

AdMMP-9 2×10^9 PFU, [###]$p < 0.0001$. (**B**) In vivo microdialysis sampling of VEGF and endostatin after AdMMP-9. No significant increases of stroma-derived (murine) VEGF and cancer cell–derived (human) VEGF were found. ANOVA, $n = 4$–8 in each group. Significant increased levels of both murine and human endostatin: *$p < 0.05$, ***$p < 0.0001$ compared with control. (**C**) Dose-dependent increase of neutrophil infiltration by AdMMP-9. *Top panel*, After immunohistochemistry, as described in the *Materials and Methods* section, the number of neutrophils was counted on tumor sections and shown to increase significantly after AdMMP-9 gene transfer in a dose-dependent fashion. Representative sections from each treatment group are depicted. $n = 12$, ANOVA, Bonferroni post hoc test. *$p < 0.05$, ***$p < 0.001$ compared with control, [#]$p < 0.05$ compared with 0.5×10^9 PFU AdMMP-9. *Bottom panel*, The chemokines KC and MIP-2 increased after AdMMP-9 treatment: $n = 6$–8 in each group, AVOVA, Bonferroni post hoc test. Scale bars, 20 μm. *$p < 0.05$, **$p < 0.01$, ***$p < 0.001$ compared with control. (**D**) In vivo cytokine profile by AdMMP-9. One week after gene transfer, microdialysis was performed to sample proteins in live tumor tissue in vivo. An M1-like cytokine profile was detected after AdMMP treatment. $n = 6$–8 in each group, ANOVA, Bonferroni post hoc test. *$p < 0.05$, **$p < 0.01$, ***$p < 0.0001$ compared with control.
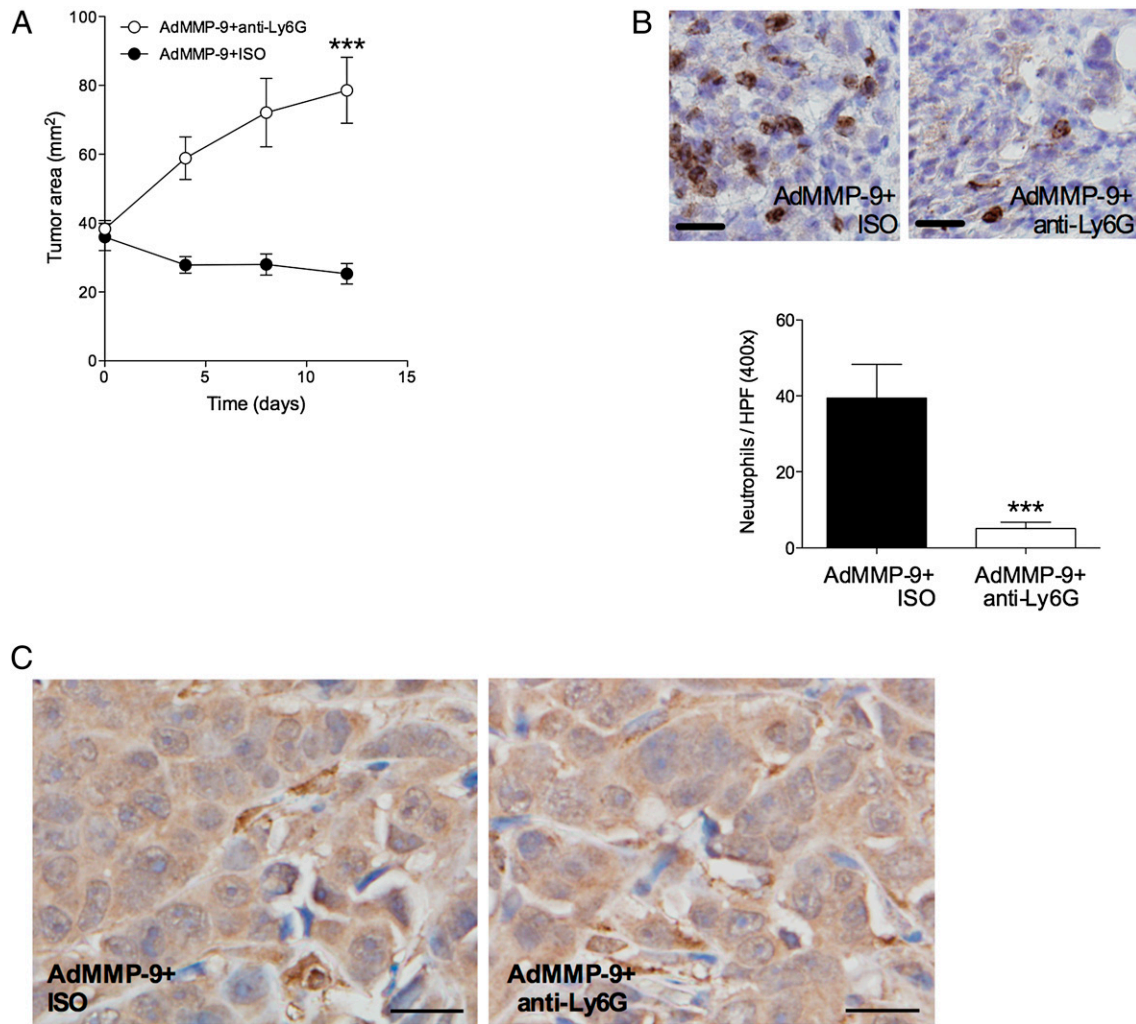
FIGURE 6. MMP-9 gene transfer induced neutrophil infiltration, and inhibition of neutrophil activity resulted in increased tumor growth. (**A**) Intratumoral injections of neutrophil-inhibiting Ab anti-Ly6G prior to AdMMP-9 gene transfer increased tumor growth significantly: $n = 7$ in each group, ***$p < 0.0001$ compared with control. (**B**) Anti-Ly6G almost completely abolished neutrophil infiltration into the tumors. Representative sections from each treatment group. Scale bars, 20 μm. $n = 7$ in each group, ***$p < 0.001$. (**C**) Immunohistochemistry of MMP-9 in presence and absence of neutrophil inhibition. There was no difference in staining intensity between the treatment groups. Representative sections from each treatment group are shown. Scale bars, 20 μm.

treme variants, and these two phenotypes may also coexist in the tumor microenvironment (45). Moreover, in the case of IL-1, this may also be a paradox because the M1 cytokine IL-1β has been shown to promote tumor angiogenesis and metastasis that may be counteracted by the M2 cytokine IL-Ra, an antagonist of IL-1 without any agonist effect (46–48). To further investigate if the

FIGURE 7. Gene transfer of MMP-9–induced tumor regression and neutrophil infiltration in immune-competent mice. FVB/n mice were oophorectomized and supplemented with a physiologic level of estradiol. MMTV-PyMT breast cancer cells were injected s.c., and tumors were formed on the right hind flank. At similar tumor sizes (~40 mm^2), intratumoral gene transfer by adenovirus was performed with Addl70-3 (empty control vector) or AdMMP-9 at 1×10^9 PFU. (**A**) Tumor growth. $n = 7$ to 8 in each group, ***$p < 0.0001$, Student t test. (**B**) AdMMP-9 resulted in significantly increased infiltration of neutrophils (anti-Ly6G) compared with the control vector group. Scale bars, 20 μm. $n = 9$ in each group, ***$p < 0.0001$, Student t test.
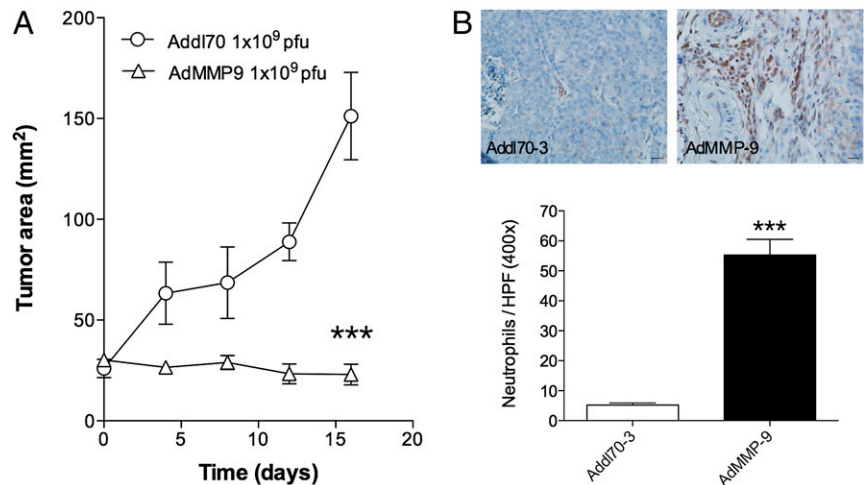
change of cytokine levels found in vivo after MMP-9 therapy could be attributable to macrophages, we cultured this cell type and exposed them to AdMMP-9. Indeed, we found that AdMMP-9 exposure to murine macrophage-like cells and freshly isolated human macrophages induced a similar cytokine profile as we had detected in the in vivo microdialysates. TNF-α was not detectable in microdialysates, but in cell culture, the macrophages responded with a prompted increase of TNF-α after AdMMP-9 therapy. This is in line with a recent study showing that two other MMPs, namely MMP-1 and MMP-3, induced a TNF-α release from macrophages (49). By blocking the PAR-1 and PAR-2 receptors in vitro, the cytokine profile was reversed, suggesting that the MMP-9 effect on the macrophages was mediated via these receptors.

AdMMP-9–treated tumors also secreted very high levels of the murine inflammatory cytokines KC and MIP-2, corresponding to human IL-8. These chemokines originated from the macrophages and neutrophils in the stroma, at least in part, as our in vitro–cultured monocytes secreted significantly increased levels of MIP-2 from murine cells and IL-8 from human cells after AdMMP-9 gene transfer. In the tumors, the high levels of KC and MIP-2 were functional, as the tumor stroma exhibited massive infiltration of neutrophils. The role of neutrophils and IL-8 in cancer progression is to some extent contradictory in previous published data. The proangiogenic IL-8 and neutrophil infiltration have been described as important mediators of transforming benign conditions into malignant lesions (44, 50); in contrast, massive infiltration of neutrophils and very high levels of IL-8 have been shown to be effective tumor-killing modalities (51). One explanation may be a dose-dependent effect, as it has been demonstrated that increasing levels of transduced IL-8 into melanoma cells caused increased tumor formation, but at very high levels of IL-8, tumor growth was impaired, dependent on massive neutrophil infiltration (26). The mechanistic explanation of such findings may be an increased production of hydrogen peroxide by the neutrophils, leading to tumor killing as recently described (52). Another recent study has also revealed that neutrophils may be activated/differentiated into an antitumorigenic or a protumorigenic phenotype (25). Depletion of these antitumor neutrophils augments tumor growth (25, 53). This is in line with our present data in which depletion of neutrophils counteracted the therapeutic effects of AdMMP-9. One strength of our experiments is that we used a highly neutrophil-specific mAb (1A8) that specifically depletes neutrophils, whereas other studies have used the RB6-8C5 Ab, which has been shown to also target a second epitope expressed on many other cell types (54). During gene transfer into tumor tissue, all cells present in the tumor at this time will overexpress the transgene, including macrophages and neutrophils. However, infiltrating cells after gene transfer will not be subjected to the viruses loaded with the transgene—in this case, MMP-9. Although neutrophils may produce MMP-9 per se, the production of MMP-9 of the incoming neutrophils after gene transfer was not high enough to sustain increased MMP-9 levels throughout the tumors, as the intensity of staining did not differ between tumors with or without depletion of neutrophils.

Although the nude mouse model gives the advantage of investigating the innate immune system exclusively, it may be argued that the antitumor effects may not be present in species with intact immunity. However, our data from the immune competent PyMT model clearly show that AdMMP-9 also exerts an antitumor activity when an intact immune system is present.

In summary, we have demonstrated several mechanisms by which AdMMP-9 exerts antitumorgenic properties in both immune-deficient and immune-competent mouse models of human breast cancer. As previously shown, AdMMP-9 increased the release of the antiangiogenic fragment endostatin. AdMMP-9 also increased the levels of KC and MIP-2 by the stroma, leading to increased influx of neutrophils into the tumor tissue. By selective depletion of neutrophils, the AdMMP-9 effects were abolished, demonstrating that these neutrophils exerted an antitumorigenic action. A large part of the tumor stroma, ~10% of the whole tumor area, consisted of macrophages in our model. Previous data have shown that the phenotype of macrophages in cancerous tissue may be reversible (55). In this study, we add MMP-9 to the complex network of molecules with abilities to activate macrophages into different functional states. Although MMP-9 did not activate the macrophages into a classic M1 tumor-killing phenotype, the cytokine profile suggested a polarization toward M1-like macrophages. Moreover, we also show that neutrophils changed their phenotype by MMP-9. Clearly, the role of MMP-9 in tumor growth is diverse, and inhibition of its activity may cause unexpected tumor response.

Disclosures

The authors have no financial conflicts of interest.

References

1. Duffy, M. J., T. M. Maguire, A. Hill, E. McDermott, and N. O'Higgins. 2000. Metalloproteinases: role in breast carcinogenesis, invasion and metastasis. *Breast Cancer Res.* 2: 252–257.
2. Stetler-Stevenson, W. G., and A. E. Yu. 2001. Proteases in invasion: matrix metalloproteinases. *Semin. Cancer Biol.* 11: 143–152.
3. Coussens, L. M., B. Fingleton, and L. M. Matrisian. 2002. Matrix metalloproteinase inhibitors and cancer: trials and tribulations. *Science* 295: 2387–2392.
4. Bendrik, C., J. Robertson, J. Gauldie, and C. Dabrosin. 2008. Gene transfer of matrix metalloproteinase-9 induces tumor regression of breast cancer in vivo. *Cancer Res.* 68: 3405–3412.
5. Hamano, Y., M. Zeisberg, H. Sugimoto, J. C. Lively, Y. Maeshima, C. Yang, R. O. Hynes, Z. Werb, A. Sudhakar, and R. Kalluri. 2003. Physiological levels of tumstatin, a fragment of collagen IV alpha3 chain, are generated by MMP-9 proteolysis and suppress angiogenesis via alphaV beta3 integrin. *Cancer Cell* 3: 589–601.
6. Nilsson, U. W., and C. Dabrosin. 2006. Estradiol and tamoxifen regulate endostatin generation via matrix metalloproteinase activity in breast cancer in vivo. *Cancer Res.* 66: 4789–4794.
7. Pozzi, A., W. F. LeVine, and H. A. Gardner. 2002. Low plasma levels of matrix metalloproteinase 9 permit increased tumor angiogenesis. *Oncogene* 21: 272–281.
8. Decock, J., S. Thirkettle, L. Wagstaff, and D. R. Edwards. 2011. Matrix metalloproteinases: protective roles in cancer. *J. Cell. Mol. Med.* 15: 1254–1265.
9. Visse, R., and H. Nagase. 2003. Matrix metalloproteinases and tissue inhibitors of metalloproteinases: structure, function, and biochemistry. *Circ. Res.* 92: 827–839.
10. Partridge, J. J., M. A. Madsen, V. C. Ardi, T. Papagiannakopoulos, T. A. Kupriyanova, J. P. Quigley, and E. I. Deryugina. 2007. Functional analysis of matrix metalloproteinases and tissue inhibitors of metalloproteinases differentially expressed by variants of human HT-1080 fibrosarcoma exhibiting high and low levels of intravasation and metastasis. *J. Biol. Chem.* 282: 35964–35977.
11. Kopitz, C., M. Gerg, O. R. Bandapalli, D. Ister, C. J. Pennington, S. Hauser, C. Flechsig, H. W. Krell, D. Antolovic, K. Brew, et al. 2007. Tissue inhibitor of metalloproteinases-1 promotes liver metastasis by induction of hepatocyte growth factor signaling. *Cancer Res.* 67: 8615–8623.
12. Lipton, A., S. M. Ali, K. Leitzel, L. Demers, D. B. Evans, P. Hamer, S. Brown-Shimer, K. Pierce, and W. Carney. 2007. Elevated plasma tissue inhibitor of metalloproteinase-1 level predicts decreased response and survival in metastatic breast cancer. *Cancer* 109: 1933–1939.
13. Miyagi, M., K. Aoyagi, S. Kato, and K. Shirouzu. 2007. The TIMP-1 gene transferred through adenovirus mediation shows a suppressive effect on peritoneal metastases from gastric cancer. *Int. J. Clin. Oncol.* 12: 17–24.
14. Klintman, M., S. Ørnbjerg Würtz, I. J. Christensen, P. Braemer Hertel, M. Fernö, M. Malmberg, H. Mouridsen, F. Cold, A. S. Schrohl, J. A. Foekens, et al. 2010. Association between tumor tissue TIMP-1 levels and objective response to first-line chemotherapy in metastatic breast cancer. *Breast Cancer Res. Treat.* 121: 365–371.
15. Schrohl, A. S., I. J. Christensen, A. N. Pedersen, V. Jensen, H. Mouridsen, G. Murphy, J. A. Foekens, N. Brunner, and M. N. Holten-Andersen. 2003. Tumor tissue concentrations of the proteinase inhibitors tissue inhibitor of metalloproteinases-1 (TIMP-1) and plasminogen activator inhibitor type 1 (PAI-1) are complementary in determining prognosis in primary breast cancer. *Mol. Cell. Proteomics* 2: 164–172.

16. Schrohl, A. S., M. P. Look, M. E. Meijer-van Gelder, J. A. Foekens, and N. Brünner. 2009. Tumor tissue levels of Tissue Inhibitor of Metalloproteinases-1 (TIMP-1) and outcome following adjuvant chemotherapy in premenopausal lymph node-positive breast cancer patients: A retrospective study. *BMC Cancer* 9: 322.

17. Rodríguez, D., C. J. Morrison, and C. M. Overall. 2010. Matrix metalloproteinases: what do they not do? New substrates and biological roles identified by murine models and proteomics. *Biochim. Biophys. Acta* 1803: 39–54.

18. Murphy, G., A. Murthy, and R. Khokha. 2008. Clipping, shedding and RIPping keep immunity on cue. *Trends Immunol.* 29: 75–82.

19. Hanahan, D., and R. A. Weinberg. 2011. Hallmarks of cancer: the next generation. *Cell* 144: 646–674.

20. Qian, B. Z., and J. W. Pollard. 2010. Macrophage diversity enhances tumor progression and metastasis. *Cell* 141: 39–51.

21. Mantovani, A., and A. Sica. 2010. Macrophages, innate immunity and cancer: balance, tolerance, and diversity. *Curr. Opin. Immunol.* 22: 231–237.

22. Movahedi, K., D. Laoui, C. Gysemans, M. Baeten, G. Stangé, J. Van den Bossche, M. Mack, D. Pipeleers, P. In't Veld, P. De Baetselier, and J. A. Van Ginderachter. 2010. Different tumor microenvironments contain functionally distinct subsets of macrophages derived from Ly6C(high) monocytes. *Cancer Res.* 70: 5728–5739.

23. Sica, A., and A. Mantovani. 2012. Macrophage plasticity and polarization: in vivo veritas. *J. Clin. Invest.* 122: 787–795.

24. Rolny, C., M. Mazzone, S. Tugues, D. Laoui, I. Johansson, C. Coulon, M. L. Squadrito, I. Segura, X. Li, E. Knevels, et al. 2011. HRG inhibits tumor growth and metastasis by inducing macrophage polarization and vessel normalization through downregulation of PlGF. *Cancer Cell* 19: 31–44.

25. Fridlender, Z. G., J. Sun, S. Kim, V. Kapoor, G. Cheng, L. Ling, G. S. Worthen, and S. M. Albelda. 2009. Polarization of tumor-associated neutrophil phenotype by TGF-beta: "N1" versus "N2" TAN. *Cancer Cell* 16: 183–194.

26. Schaider, H., M. Oka, T. Bogenrieder, K. Nesbit, K. Satyamoorthy, C. Berking, K. Matsushima, and M. Herlyn. 2003. Differential response of primary and metastatic melanomas to neutrophils attracted by IL-8. *Int. J. Cancer* 103: 335–343.

27. Dabrosin, C., P. J. Margetts, and J. Gauldie. 2003. Estradiol increases extracellular levels of vascular endothelial growth factor in vivo in murine mammary cancer. *Int. J. Cancer* 107: 535–540.

28. Dabrosin, C., K. Palmer, W. J. Muller, and J. Gauldie. 2003. Estradiol promotes growth and angiogenesis in polyoma middle T transgenic mouse mammary tumor explants. *Breast Cancer Res. Treat.* 78: 1–6.

29. Bramson, J. L., F. L. Graham, and J. Gauldie. 1995. The use of adenoviral vectors for gene therapy and gene transfer in vivo. *Curr. Opin. Biotechnol.* 6: 590–595.

30. Lewis, C. E., M. De Palma, and L. Naldini. 2007. Tie2-expressing monocytes and tumor angiogenesis: regulation by hypoxia and angiopoietin-2. *Cancer Res.* 67: 8429–8432.

31. Colognato, R., J. R. Slupsky, M. Jendrach, L. Burysek, T. Syrovets, and T. Simmet. 2003. Differential expression and regulation of protease-activated receptors in human peripheral monocytes and monocyte-derived antigen-presenting cells. *Blood* 102: 2645–2652.

32. Lee, E. J., M. S. Woo, P. G. Moon, M. C. Baek, I. Y. Choi, W. K. Kim, E. Junn, and H. S. Kim. 2010. Alpha-synuclein activates microglia by inducing the expressions of matrix metalloproteinases and the subsequent activation of protease-activated receptor-1. *J. Immunol.* 185: 615–623.

33. López-Otín, C., and L. M. Matrisian. 2007. Emerging roles of proteases in tumour suppression. *Nat. Rev. Cancer* 7: 800–808.

34. Martin, M. D., and L. M. Matrisian. 2007. The other side of MMPs: protective roles in tumor progression. *Cancer Metastasis Rev.* 26: 717–724.

35. Coussens, L. M., C. L. Tinkle, D. Hanahan, and Z. Werb. 2000. MMP-9 supplied by bone marrow-derived cells contributes to skin carcinogenesis. *Cell* 103: 481–490.

36. Pellikainen, J. M., K. M. Ropponen, V. V. Kataja, J. K. Kellokoski, M. J. Eskelinen, and V. M. Kosma. 2004. Expression of matrix metalloproteinase (MMP)-2 and MMP-9 in breast cancer with a special reference to activator protein-2, HER2, and prognosis. *Clin. Cancer Res.* 10: 7621–7628.

37. Schäfer, S., S. Weibel, U. Donat, Q. Zhang, R. J. Aguilar, N. G. Chen, and A. A. Szalay. 2012. Vaccinia virus-mediated intra-tumoral expression of matrix metalloproteinase 9 enhances oncolysis of PC-3 xenograft tumors. *BMC Cancer* 12: 366.

38. Bergers, G., R. Brekken, G. McMahon, T. H. Vu, T. Itoh, K. Tamaki, K. Tanzawa, P. Thorpe, S. Itohara, Z. Werb, and D. Hanahan. 2000. Matrix metalloproteinase-9 triggers the angiogenic switch during carcinogenesis. *Nat. Cell Biol.* 2: 737–744.

39. Dabrosin, C. 2003. Increase of free insulin-like growth factor-1 in normal human breast in vivo late in the menstrual cycle. *Breast Cancer Res. Treat.* 80: 193–198.

40. Dabrosin, C. 2005. Microdialysis - an in vivo technique for studies of growth factors in breast cancer. *Front. Biosci.* 10: 1329–1335.

41. Dabrosin, C. 2005. Positive correlation between estradiol and vascular endothelial growth factor but not fibroblast growth factor-2 in normal human breast tissue in vivo. *Clin. Cancer Res.* 11: 8036–8041.

42. Dabrosin, C., A. Hallström, U. Ungerstedt, and M. Hammar. 1997. Microdialysis of human breast tissue during the menstrual cycle. *Clin. Sci.* 92: 493–496.

43. Dabrosin, C., K. Ollinger, U. Ungerstedt, and M. Hammar. 1997. Variability of glutathione levels in normal breast tissue and subcutaneous fat during the menstrual cycle: an in vivo study with microdialysis technique. *J. Clin. Endocrinol. Metab.* 82: 1382–1384.

44. Bendrik, C., and C. Dabrosin. 2009. Estradiol increases IL-8 secretion of normal human breast tissue and breast cancer in vivo. *J. Immunol.* 182: 371–378.

45. Biswas, S. K., and A. Mantovani. 2010. Macrophage plasticity and interaction with lymphocyte subsets: cancer as a paradigm. *Nat. Immunol.* 11: 889–896.

46. Voronov, E., D. S. Shouval, Y. Krelin, E. Cagnano, D. Benharroch, Y. Iwakura, C. A. Dinarello, and R. N. Apte. 2003. IL-1 is required for tumor invasiveness and angiogenesis. *Proc. Natl. Acad. Sci. USA* 100: 2645–2650.

47. Lindahl, G., N. Saarinen, A. Abrahamsson, and C. Dabrosin. 2011. Tamoxifen, flaxseed, and the lignan enterolactone increase stroma- and cancer cell-derived IL-1Ra and decrease tumor angiogenesis in estrogen-dependent breast cancer. *Cancer Res.* 71: 51–60.

48. Dinarello, C. A. 2010. Why not treat human cancer with interleukin-1 blockade? *Cancer Metastasis Rev.* 29: 317–329.

49. Steenport, M., K. M. Khan, B. Du, S. E. Barnhard, A. J. Dannenberg, and D. J. Falcone. 2009. Matrix metalloproteinase (MMP)-1 and MMP-3 induce macrophage MMP-9: evidence for the role of TNF-alpha and cyclooxygenase-2. *J. Immunol.* 183: 8119–8127.

50. Tazawa, H., F. Okada, T. Kobayashi, M. Tada, Y. Mori, Y. Une, F. Sendo, M. Kobayashi, and M. Hosokawa. 2003. Infiltration of neutrophils is required for acquisition of metastatic phenotype of benign murine fibrosarcoma cells: implication of inflammation-associated carcinogenesis and tumor progression. *Am. J. Pathol.* 163: 2221–2232.

51. Lee, L. F., R. P. Hellendall, Y. Wang, J. S. Haskill, N. Mukaida, K. Matsushima, and J. P. Ting. 2000. IL-8 reduced tumorigenicity of human ovarian cancer in vivo due to neutrophil infiltration. *J. Immunol.* 164: 2769–2775.

52. Granot, Z., E. Henke, E. A. Comen, T. A. King, L. Norton, and R. Benezra. 2011. Tumor entrained neutrophils inhibit seeding in the premetastatic lung. *Cancer Cell* 20: 300–314.

53. Colombo, M. P., L. Lombardi, A. Stoppacciaro, C. Melani, M. Parenza, B. Bottazzi, and G. Parmiani. 1992. Granulocyte colony-stimulating factor (G-CSF) gene transduction in murine adenocarcinoma drives neutrophil-mediated tumor inhibition in vivo. Neutrophils discriminate between G-CSF-producing and G-CSF-nonproducing tumor cells. *J. Immunol.* 149: 113–119.

54. Daley, J. M., A. A. Thomay, M. D. Connolly, J. S. Reichner, and J. E. Albina. 2008. Use of Ly6G-specific monoclonal antibody to deplete neutrophils in mice. *J. Leukoc. Biol.* 83: 64–70.

55. Stout, R. D., S. K. Watkins, and J. Suttles. 2009. Functional plasticity of macrophages: in situ reprogramming of tumor-associated macrophages. *J. Leukoc. Biol.* 86: 1105–1109.